ELSEVIER

Thermochimica Acta 292 (1997) 85–94

thermochimica acta

Catalytic reduction of carbon–chromite composite pellets by lime

Y.L. Ding*, N.A. Warner

School of Chemical Engineering, The University of Birmingham, Edgbaston, Birmingham B15 2TT, UK

Received 25 July 1996

Abstract

The catalytic effect of lime on the reduction of carbon–chromite composite pellets was investigated at 1270–1433°C under CO-argon atmospheres. It was found that the data for the early stage of reduction, up to a reduction level of 30–60%, fit both an exponential law for nucleation control and an equation for chemical control with an apparent activation energy ranging from 139 to 161 kJ/mol depending on the amount of lime addition. In the late stage (after about 65% reduction), solid diffusion of chromium in the oxide phase is the most likely rate-controlling step with an apparent activation energy of 410 kJ/mol. Besides the possibility of it being able to go into the spinel lattice and release the FeO, lime is also suggested to catalyse the chromite reduction through enhancing the nucleation and/or interfacial reaction in the early stage, and facilitating the solid-diffusion process in the late stage. The results of this study also indicate that heat treatment of chromite has a significant effect on the reduction kinetics. © 1997 Elsevier Science B.V.

Keywords: Carbothermic reduction; Chromite; Flux; Rate-controlling steps

1. Introduction

Ferrochromium is one of the most important alloying materials used in the production of stainless and high-alloying ferritic steels. At present, high carbon ferrochromium is mainly produced in submerged-arc furnaces. Disadvantages of this process are the limited use of chromite fines and friable chrome ores, as well as its dependence on both expensive metallurgical coke and electrical energy. To improve the cost effectiveness, carbothermic prereduction has gained importance.

The carbothermic reduction of chromite in the presence of fluxes has been a subject of several investigations [1–7]. The published information on the effect of lime, however, is very limited. Sundar Murti et al. investigated the effect of 8% CaO on the reduction of both synthetic and natural chromites by graphite at 1200–1300°C [6]. They found that the reduction was enhanced by the additive and attributed this enhancement to the lime going into the spinel lattice and releasing the FeO, thereby increasing the chromite reducibility. Van Deventer studied the effect of the amount of lime addition on the reduction of Kroondal chromite by graphite at 1400°C [7]. The reduction rate and extent were found to increase all the way with increasing lime addition up to 15% with respect to chromite. Besides the possibility that the lime may enter the spinel lattice with the release of FeO component, the positive effect of lime was also attributed to its catalytic influence on the Boudouard reaction.

*Corresponding author. Tel.: 021-414-5383; fax: 0044-121-414-5378.

PII S0040-6031(97)00050-6

There is no doubt about the catalytic effect of lime on the chromite reduction. A careful examination of the interpretations by the previous investigators raises two questions. Firstly, because iron is reduced preferentially during the chromite reduction [5,7], if lime affects the reduction only through entering the spinel lattice and releasing the FeO component, the effect would be confined to the early stage of reduction. The experiments conducted by these investigators, however, show that the effect of lime lasted throughout the whole reduction process. Secondly, because the Boudouard reaction is very unlikely to be rate controlling at above 1270°C, as will be seen later on, the catalytic effect of lime on this reaction is unimportant to the reduction kinetics.

The objective of this study is directed at the establishment and understanding of the kinetics and mechanism of chromite reduction in the presence of lime. The carbon–chromite pellets are used in this study. This is believed to be more important from the viewpoint of making use of chromite fines and friable chrome ores, since agglomeration is necessary for these ores before being fed into the submerged-arc furnaces.

2. Experimental

2.1. Pellet preparation

The cylindrical pellets used in this study were made up of ground South African chromite concentrate, high-grade graphite powder (Aldrich Chemicals) and reagent grade CaO (98%, Aldrich Chemicals). The chromite contained 39.6%Cr_2O_3, 23.7%Fe_2O_3, 14.6%MgO, 15.2%Al_2O_3, 5.8%SiO_2, 0.4%CaO and 0.22%MnO. The calculated Cr/Fe ratio of the chromite was 1.635. The mean diameters of chromite and graphite were 100 μm and 1.5 μm, respectively.

The pellets were 10 mm in both diameter and height. They were formed by the compaction of thoroughly-mixed chromite, graphite and lime in a steel die under a pressure of 22 MPa. One drop of water was used as the binder for each pellet. The weight ratio of graphite to chromite in the composite pellets was 0.21, which was about 10% in excess of the stoichiometric requirement for the reduction of chromium and iron oxides to the M_7C_3-type carbides. Due to the hygroscopic nature of lime and its reaction with CO_2 in the air, the chromite and predetermined amount of lime was mixed thoroughly and heated to 1200°C in a muffle furnace for 2 h before the pellet production. In addition, some green pellets were also made to examine the effect of heat treatment. The pellets were dried at 110°C for 3 h to remove the moisture and were kept in a desiccator for the reduction experiments.

2.2. Equipment and techniques

The experimental equipment consists of a water-cooled brass outer casing that stood 360 mm high and was 220 mm in diameter at its widest point (Fig. 1). A dense graphite crucible was used as susceptor, which was insulated by various layers of refractory. A recrystallized alumina crucible with an inner diameter of 45 mm and a height of 70 mm was held within the graphite crucible. There is a gas outlet and an inert gas/vacuum inlet on the lid of the equipment. The whole rig was sealed so that it can be evacuated and an atmosphere of argon can be introduced into the system. The gas outlet was connected to a dial type total volume meter via a tubular heat exchanger. This ensured that the reaction gas can be cooled to the ambient temperature as required by the gas meter. The pellets were magnetically delivered via a glass side-arm sealed in one end by a sprung ground glass joint. The induction current was generated by a high frequency 12 kVA Cheltenham Induction Unit. The temperature of the graphite crucible was measured by a Type R Pt/Pt-Rh thermocouple and controlled by an Eurotherm 812 digital controller. The progress of the experiment was monitored with a video camera via a glass prism placed on the top of the sight hole. The sight hole was also used for measuring (calibrating) the temperature of the alumina crucible by another Pt/Pt-Rh thermocouple, since what the controller detected was the temperature of the graphite crucible.

In a typical run of the experiments, the system was repeatedly evacuated and backfilled with argon. Power was then turned on to supply heat to the rig gradually. Argon flushing was kept during heating up. When the temperature reached the predetermined value, tem-

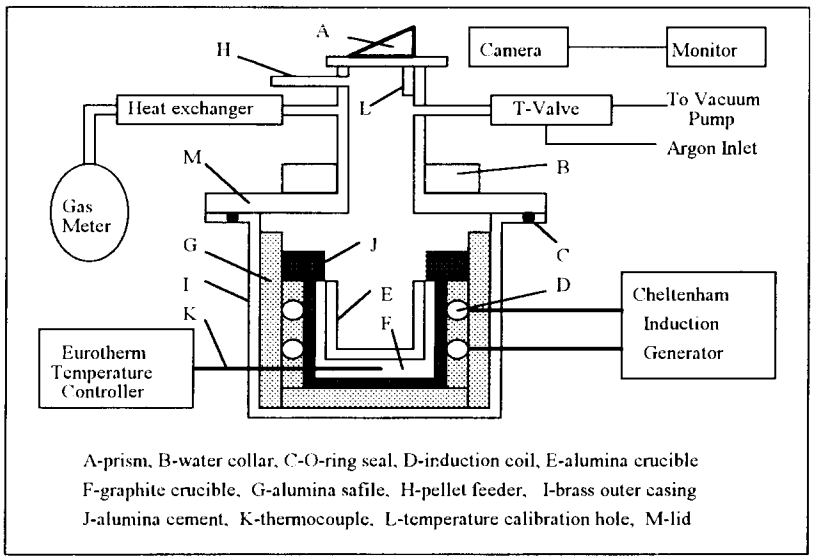

Fig. 1. Experimental system.

perature calibration was conducted, during which argon flowrate was increased. On completion of the temperature calibration, argon flow was cut off and blank experiment was carried out to correct the experimental results. Two pellets, which had been previously dried at 110°C for 3 h, were then dropped down into the alumina crucible. As the pellets hit the bottom of the alumina crucible, the stopwatch was started and gas evolution readings taken. By assuming that the composition of the gaseous reduction product is CO, the reduction fraction can then be calculated from the following equation:

$$F(t) = [V(t) - V_B(t)]/Vt \quad (1)$$

where, $F(t)$ denotes the reduction fraction, $V(t)$ the total gas evolution in time t obtained in the reduction process, $V_B(t)$ the total gas evolution in time t taken in the blank experiment, and Vt the total theoretical gas evolution for complete reduction of iron and chromium oxides in the pellets to the metallic state. Experimental results show that $V_B(t)$ depends on the reduction temperature and ranges from 10^{-5} to 10^{-4} dm^3/min. This is negligible compared with the gas evolution of the reduction reaction. After the experiments, some reduced pellets were subjected to X-Ray diffraction to identify the reaction products.

3. Results

3.1. Effect of amount of lime addition

The effect of amount of lime on the reduction kinetics was tested with 4 lime additions, i.e. 0.4% (base condition), 5.18%, 9.54% and 13.52% with respect to chromite. Figs. 2–5 show the experimental results. The reduction rate and extent increase with increasing lime addition at all temperatures investigated. After a reduction for 10 min, an increase in the lime addition from 0.4% to 13.52% results in an increase in the reduction fraction by 12% at 1270°C, by 36% at 1328°C, by 24% at 1388°C and by 26% at 1433°C.

3.2. Effect of temperature

The effect of temperature on the reduction kinetics was examined at 1270, 1328, 1388 and 1433°C. Fig. 6 shows the results with a lime addition of 9.54%. It is seen that the reduction is obviously favoured by high temperatures. At and above 1328°C, the reduction can be expected to finish in about 10–20 min. A comparison of Figs. 2–5 also suggests that the effect of lime is more significant at low temperatures. For a given temperature, the effect of lime is more marked in

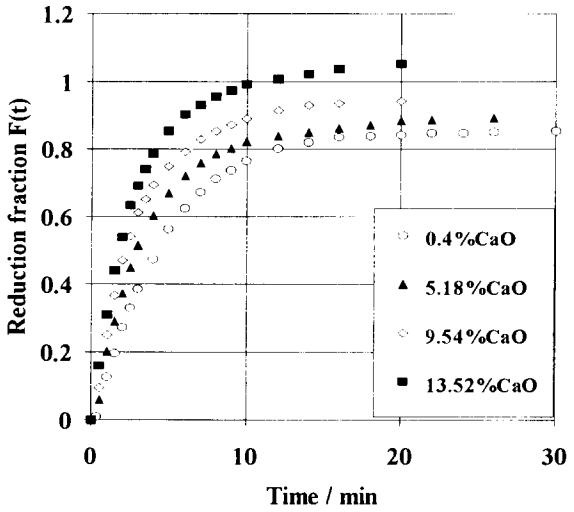

Fig. 2. Effect of lime addition at 1433°C.

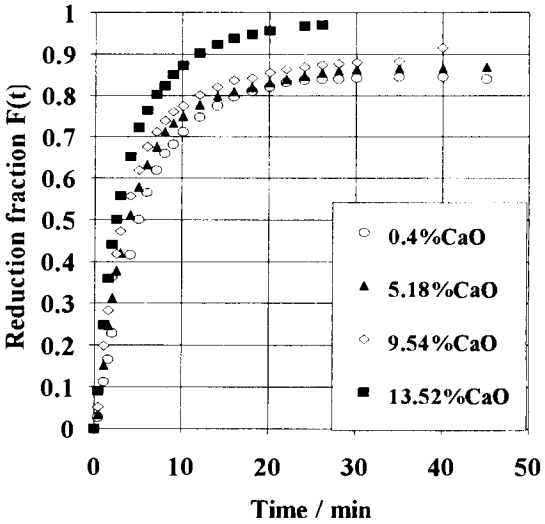

Fig. 3. Effect of lime addition at 1388°C.

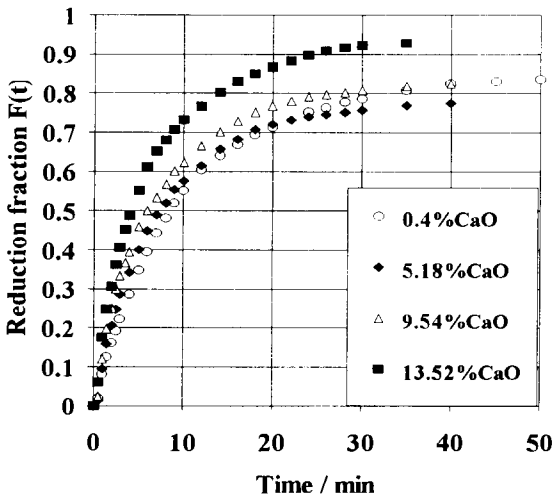

Fig. 4. Effect of lime addition at 1328°C.

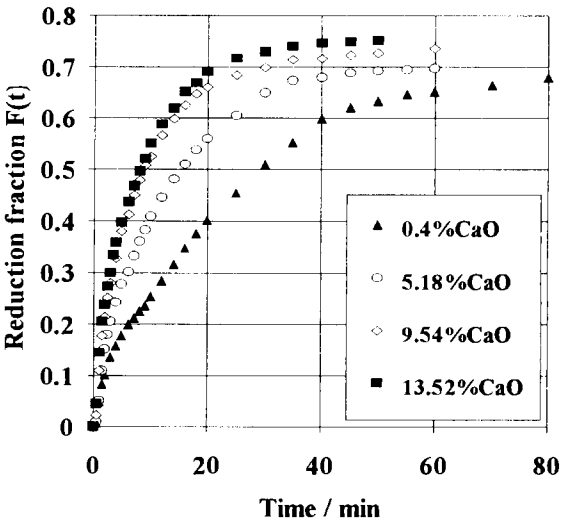

Fig. 5. Effect of lime addition at 1270°C.

the early stage of reduction. At 1433°C, a reduction fraction slightly greater than 1 can be seen from Fig. 1. This is due to the reduction of a small amount of silica, which is not included in Eq. (1). It should be noted that, according to the thermodynamic calculation, lime cannot be reduced under the conditions of this study. This was also confirmed by the X-Ray diffraction analyses on the reduced pellets.

3.3. *Effect of heat treatment*

Fig. 7 shows the effect of heat treatment of chromite ore on the reduction kinetics at 1270°C. In this figure, HT denotes that the chromite ore was heated to 1200°C for 2 h before the pellets were made, NHT stands for no heat treatment, i.e. green pellets were used. It is seen that heat treatment can improve the

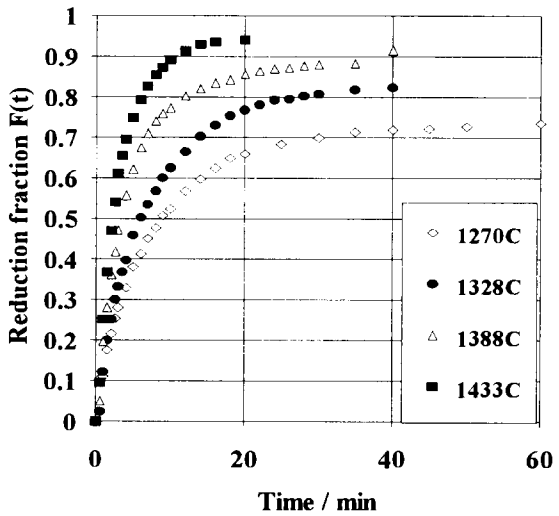

Fig. 6. Effect of temperature (9.54% CaO).

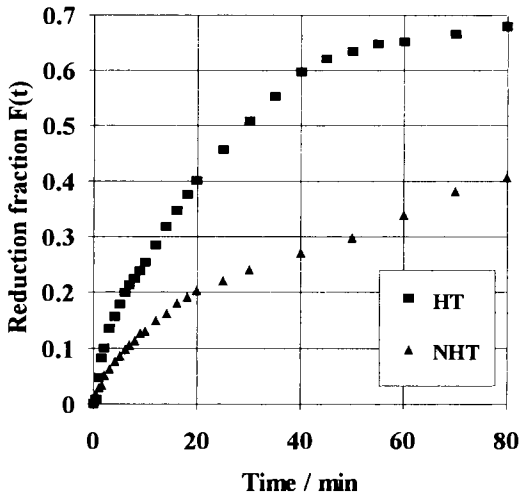

Fig. 7. Effect of heat treatment at 1270°C.

reducibility of chromite. This is in agreement with that obtained by Fernandes et al. [8].

4. Discussions

4.1. Initial rate of reduction

Table 1 shows the initial rate of reduction (k_i) calculated from the regression expression of the experimental data. By using an Arrhenius equation, the apparent activation energy based on the initial rate (E_i) can be obtained (Table 1). It is seen that the initial rate of reduction increases with increasing reduction temperature and lime addition. The apparent activation energy, however, decreases with increasing lime addition, indicating that lime has a catalytic effect on the chromite reduction. The activation energy E_i for 0.4% CaO obtained in this study (142 kJ/mol) is comparable with that obtained in a previous study (118 kJ/mol) [9]. The difference may be explained by the effect of heat treatment, which alters the microstructures of chromite grains [8]. Another possible reason is the oxidation of some divalent iron ions to the trivalent state, which enhances the reducibility of chromite.

4.2. Boudouard reaction control

Van Deventer attributed the positive effect of lime on the carbothermic reduction of chromite at 1400°C to its catalytic influence on the Boudouard reaction [6]. The following three reasons, however, suggest that the Boudouard reaction is very unlikely to be rate controlling under the conditions of this study. Firstly, the reduction of chromite may proceed via solid–solid reaction as suggested by Barcza et al. [10] or via gaseous intermediates CO and CO_2 as proposed by

Table 1
Initial rate and apparent activation energy based on the initial rate

CaO/%	k_i/s^{-1}				E_i/kJ/ mol
	1270/°C	1328/°C	1388/°C	1433/°C	
0.4	8.03E-4	1.34E-3	1.86E-3	2.90E-3	142
5.18	8.37E-4	1.57E-3	2.56E-3	3.36E-3	154
9.54	1.83E-3	2.01E-3	3.29E-3	4.20E-3	104
13.52	2.42E-3	2.94E-3	4.14E-3	5.16E-3	84

Rankin [11]. Only in the later case, can the reduction be controlled by the Boudouard reaction. However, the reduction temperature in this study ranges from 1270 to 1433°C, at which the Boudouard reaction can take place very rapidly [12–14]. Secondly, because iron oxide is reduced preferentially during the chromite reduction [5,11], if the Boudouard reaction were rate limiting, the following reaction would be close to equilibrium [12]:

$$Fe_2O_3 + CO = 2FeO + CO_2 \quad (2)$$

and there would be an appreciable amount of CO_2 in the gaseous reduction products [12]. The gaseous reduction products, however, were found to overwhelmingly contain CO [7,15]. Finally, because CaO has been shown to have a catalytic effect on the oxidation of carbon by CO_2 [6,16,17], if Boudouard reaction were rate controlling, the apparent activation energy based on the initial reduction rate would be very close to the value for the Boudouard reaction. The apparent activation energy based on the initial reduction rate (84–142 kJ/mol), however, differs considerably from that for the Boudouard reaction (~256 kJ/mol [16]).

4.3. *Nucleation control and chemical reaction control*

It was found that the following equation can be used to fit the data of the early stage of reduction up to a reduction level of about 30–60% depending on both the reduction temperature and amount of lime addition:

$$Y_n = -\ln[1 - F(t)] = k_n \cdot t \quad (3)$$

Eq. (3) is the kinetic model for nucleation control [4]. k_n is the rate constant (s^{-1}). Fig. 8(a) and Fig. 8(b) show the typical plots of Y_n against time for the reduction at 1433 and 1328°C, respectively. It can

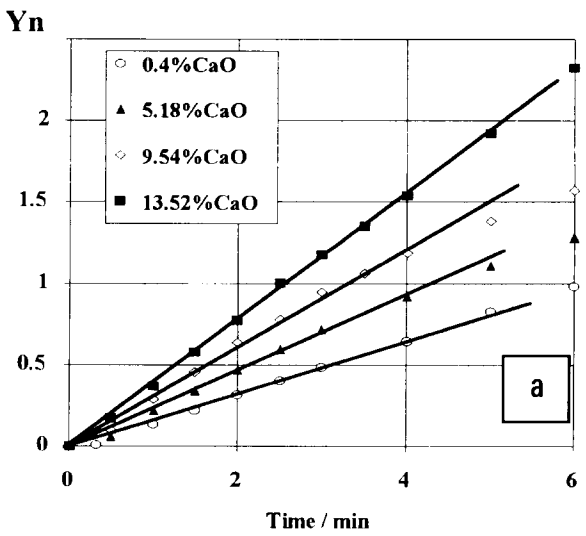

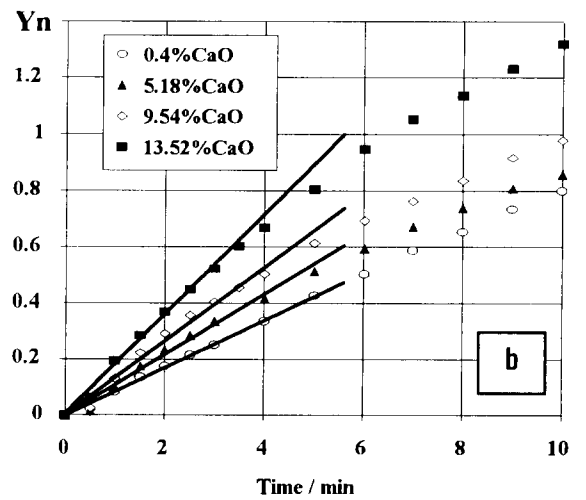

Fig. 8. Plots for nucleation control: (a) 1433°C; (b) 1328°C.

Table 2
Rate constant and apparent activation energy for nucleation control (early stage)

CaO/%	k_n/s^{-1}				E_n/kJ/mol
	1270/°C	1328/°C	1388/°C	1433/°C	
0.4	8.33E-4	1.33E-3	2.42E-3	2.78E-3	161
5.18	1.25E-3	1.82E-3	3.08E-3	3.67E-3	150
9.54	1.91E-3	2.22E-3	3.57E-3	5.13E-3	141
13.52	2.29E-3	2.86E-3	4.58E-3	6.67E-3	139

be seen that linear relationship between Y_n and time is evident in the early stage of reduction. The slopes of the linear part of the plots can be used to calculate the rate constant k_n, which in turn can be used to estimate the apparent activation energy E_n by using an Arrhenius equation. Table 2 shows the results. It is seen that the addition of lime results in a considerable increase in the rate constant. The apparent activation energy, however, changes only slightly with increasing lime addition. This indicates that lime does not change the rate-limiting step in the early stage of reduction. The apparent activation energy for 0.4% CaO (161 kJ/mol) is comparable with that obtained in a previous study (172 kJ/mol) [9].

Because of approximately constant ratio of $Y_{ch} = 1 - [1 - F(t)]^{1/3}$ (kinetic model for chemical control) to $Y_n = -\ln[1 - F(t)]$ in the early stage of reduction (~0.33) [18], the relationship between Y_{ch} and time is also linear in this stage (Fig. 9). Thus, the early stage of reduction is most likely to be controlled by either or both of nucleation and chemical reaction.

4.4. Solid-diffusion control

The data for the late stage of the reduction, after a reduction level of about 65%, were found to fit the following Zhuravlev–Lesokhin–Tempel'man equation [18,19]:

$$Y_{sd} = \{1/[1 - F(t)]^{1/3} - 1\}^2 = k_{sd} \cdot t \qquad (4)$$

Eq. (4) is the kinetic model for solid-diffusion control. k_{sd} is the rate constant (s^{-1}). Fig. 10 shows the typical plots of Y_{sd} against time for the reduction at 1433°C. Listed in Table 3 are the rate constants (k_{sd}) calculated from the slopes of the linear part of the plots, and the apparent activation energy (E_{sd}) estimated from the rate constant k_{sd}. It can be seen that the rate constant for solid-diffusion control increases with increasing temperature and lime addition. The apparent activation energy, however, is almost independent of the lime addition, indicating that lime does not change the rate-limiting step in the late stage of reduction.

4.5. Reduction mechanism

Sundar Murti et al. attributed the effect of lime to its going into the spinel lattice and releasing the FeO,

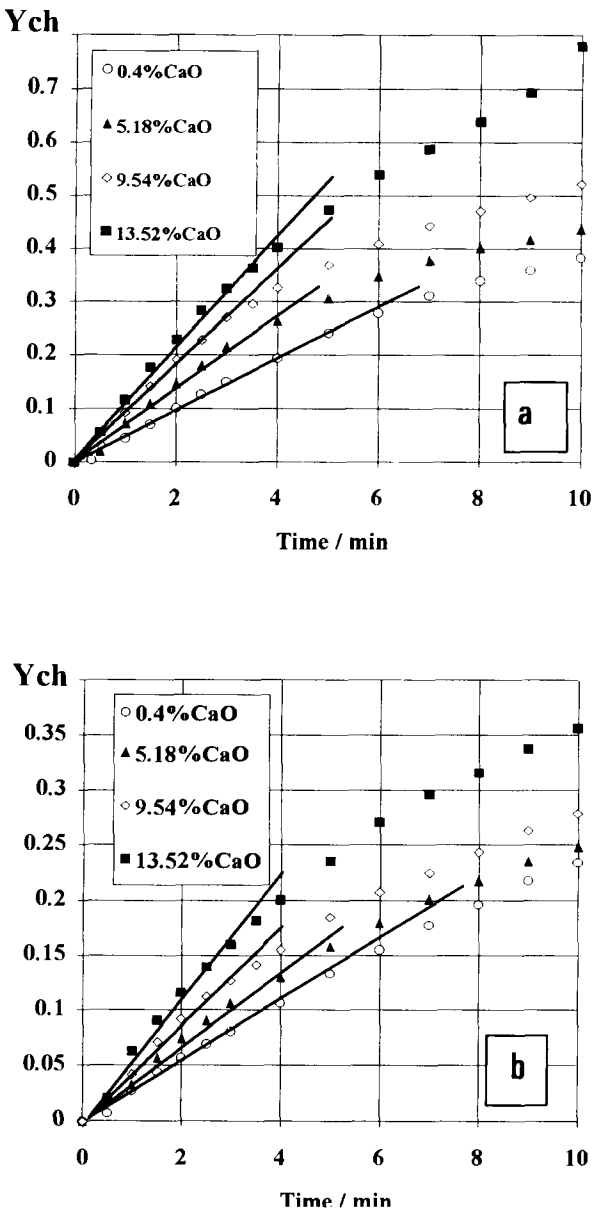

Fig. 9. Plots for chemical control: (a) 1433°C; (b) 1328°C.

thereby increasing the reducibility of chromite [7]. Van Deventer ascribed the effect of lime to it catalysing the Boudouard reaction [6]. Because the Boudouard reaction is very unlikely to be rate controlling, the following discussion focuses on the viewpoint of Sundar Murti et al. [7].

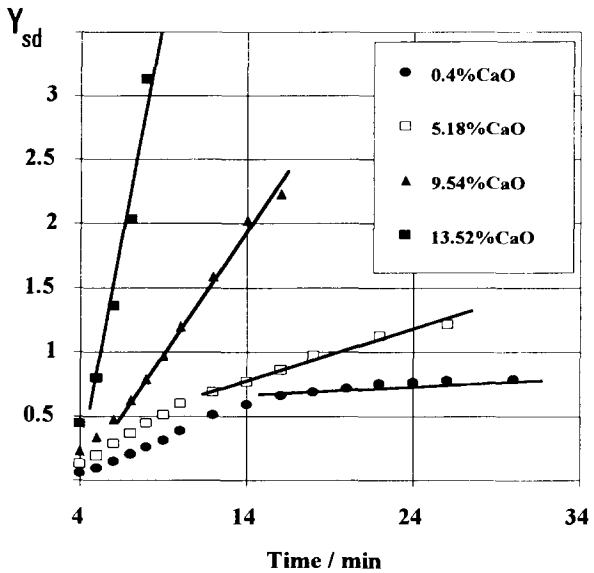

Fig. 10. Plots for solid-diffusion control at 1433°C.

The formula of chromite used in this study can be written as:

$$(Fe_{2.12}Mg_{5.88})[Cr_{8.46}Fe_{2.70}Al_{4.84}]O_{32} \quad (5)$$

where ( ) and [ ] refer to tetrahedral and octahedral coordination, respectively. This formula is based on the assumption that the spinel is stoichiometric [20]. Considering the following reaction between chromite and lime:

$$(Fe_{2.12}Mg_{5.88})[Cr_{8.46}Fe_{2.70}Al_{4.84}]O_{32} + 2.12CaO = 2.12FeO + (Ca_{2.12}Mg_{5.88})[Cr_{8.46}Fe_{2.70}Al_{4.84}]O_{32} \quad (6)$$

it can be concluded that 0.081 g of CaO are required to release all the divalent iron ions from the spinel lattice for 1 g chromite ore, i.e. 8.1% CaO with respect to chromite ore. This means that if lime affected the reduction only through its going into the spinel lattice and releasing FeO, a lime addition of greater than 8.1% would not make much difference in the reduction rate and extent from that of 8.1%, and the effect of lime would only last to the completion of iron reduction (about 36%). The experimental results, however, show that an increase in lime addition from 9.54% to 13.52% still leads to a considerable increase in both the reduction rate and extent (Figs. 2–5). Thus, besides the mechanism proposed by Sundar Murti et al. [7], there must exist other mechanisms that lime can enhance the carbothermic reduction of chromite.

It has been reported that CaO has no effect on the gaseous reduction of iron oxides [21]. In view of the Boudouard reaction being not rate limiting, it can be concluded that carbothermic reduction of chromite with a lime addition is most likely to proceed via solid–solid reaction rather than via CO and CO_2 as intermediates under the conditions of this study. This is in agreement with that suggested by Barcza et al. [10].

The process of low grade chromite reduction without any flux has been identified to include two stages [5,20,22]. The first stage is primarily confined to iron metallization. The second stage is confined to chromium reduction. For the chromite reduction with a lime addition, due to lime being able to enter the spinel lattice and release the FeO from the tetrahedral sites, the whole reduction process can be considered to include three stages. The first stage is confined to the reduction of iron oxide released by lime, which is faster than the reduction of the divalent iron in the spinel lattice. For the case of lime addition being more than that required for releasing all the FeO from the spinel lattice, the remaining lime seems to have a

Table 3
Rate constant and apparent activation energy for solid diffusion (late stage)

CaO/%	k_{sd}/s^{-1}				E_{sd}/kJ/mol
	1270/°C	1328/°C	1388/°C	1433/°C	
0.4	6.45E-5	2.76E-4	5.77E-5	1.25E-4	400
5.18	1.00E-5	3.20E-5	6.83E-4	1.34E-4	350
9.54	1.80E-5	4.00E-4	8.29E-4	3.33E-3	395
13.52	2.50E-5	1.11E-3	3.70E-4	9.45E-3	487

catalytic effect on the iron reduction by solid carbon. The experimental results support this conclusion (Figs. 2–5). As has been discussed previously, the first stage is very likely to be controlled by nucleation and/or chemical reaction. Lime may improve nucleation and/or chemical reaction in this stage, but it does not change the rate-controlling step. Soykan et al. investigated the mechanism of chromite reduction by graphite at 1416°C [23]. Interfacial reaction was found to be rate limiting in the early stage up to about 40% reduction. Taneka and Robertson heated carbon–chromite composite pellets at 1350–1750°C under both argon and CO atmospheres [4]. Nucleation was found to control the early stage of reduction under argons with an apparent activation energy of 167 kJ/mol. These findings also support the foregoing proposed mechanism.

The second stage is mainly confined to the reduction of the remaining iron in the spinel and the third stage to the chromium reduction. Microscopic study on the reduced chromite grains of both low grade (Cr/Fe~1.5) [5,20,22] and high grade (Cr/Fe~3.5) [24,25] reveals that inward diffusion of Cr^{2+} and outward diffusion of Cr^{3+} and Fe^{2+} occur during reduction. The results of this study suggest that the reduction proceeds via solid carbon. Thus, the reduction in the second and third stages can be postulated to involve the following steps (Fig. 11):

Step 1 – (a) Inward transport of carbon and (b) outward transport of Fe^{2+} and Cr^{3+} to the interface between the carbide layer and reduced area (Interface I).

Step 2 – Reaction at the interface I.

$$Fe^{2+}O^{2-} + C = Fe + CO \quad (7)$$

$$Cr^{3+} + (1/2)O^{2-} + (1/2)C = Cr^{2+} + (1/2)CO \quad (8)$$

$$Cr^{2+} + O^{2-} + C = Cr + CO \quad (9)$$

Step 3 – Outward transport of CO.

Step 4 – Inward transport of Cr^{2+} to the interface between the unreduced core and reduced area (Interface II).

Step 5 – Reaction at the interface II.

$$Cr^{2+} + Fe^{3+} = Fe^{2+} + Cr^{3+} \quad (10)$$

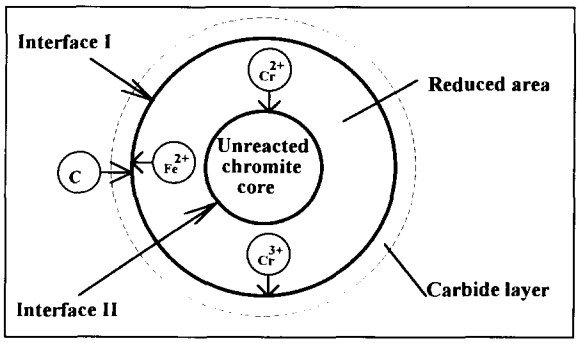

Fig. 11. Schematic diagram of the reduction mechanism of chromite.

It is obvious that the above stage wise mechanism occurs simultaneously, and the oxygen is removed from the Interface I. This is similar to the mechanism described by Soykan et al. [20,23]. In view of the linear relationship between Y_{sd} and time after a reduction level of about 65%, it can be concluded that solid-diffusion (steps 1 and 4) is very likely to be the rate-controlling step in the third stage (iron has already been reduced after 65% reduction). As has been given in Table 3, the apparent activation energy for the solid diffusion control is about 410 kJ/mol. This energy barrier is rather high for the diffusion of carbon through the carbide layer into the Interface I. In consideration of the much larger radius of chromium atoms when compared with that of carbon atoms, it can be concluded that the solid diffusion of chromium in the oxide phase is the most likely rate-controlling step. The rate-controlling step in the second stage cannot be drawn from the experimental results, it seems that the solid-diffusion and nucleation and/or chemical reaction are very likely to lead to mixed control in this stage.

Because the carbon–chromite composite pellets were used in this study, the outward transport of gaseous reduction products from inside the pellets may affect the reduction kinetics. Observation was therefore made on the reduced pellets. It was found that there are many radial cracks (~0.2 mm wide) on the curved surface of the pellets with high lime additions reduced at high temperatures (1433 and 1388°C). These cracks did not occur in the reduction of chromite pellets without lime addition [9,18]. There are two reasons that may cause these cracks. One is the

uneven stress formed during the pellet preparation. The other is the rapid evolution of gaseous reduction products from inside the pellets. In view of no evident cracks on the surface of pellets reduced at lower than 1328°C, it can be concluded that the later reason is the main one. The presence of the relative large cracks suggests that the outward transport of gaseous reduction products is very unlikely to be rate controlling. This is in agreement with the theoretical prediction [18].

5. Conclusions

Experiments on the catalytic reduction of carbon–chromite composite pellets by lime were carried out at 1270–1433°C with an inductively heated test rig under argon-CO atmospheres. The reduction rate and extent were found to increase with increasing reduction temperature and lime addition. The effect of lime was more significant at low temperatures. For a given temperature, a more remarkable effect of lime was observed in the early stage of reduction. Heat treatment of chromite ore significantly affected the reduction kinetics, and may be explained by the change in the microstructures and oxidation of the divalent iron to the trivalent state (thereby enhancing the chromite reducibility).

Under the conditions of this study, chromite reduction is very likely to proceed via solid–solid reaction rather than via CO and CO_2 as intermediates. Outward transport of gaseous reduction products from inside the composite pellets is unlikely to be rate limiting due to the formation of radial cracks on the curved surface of the pellets.

A three-stage reduction mechanism was proposed. The first stage is confined to the reduction of iron oxide released by lime. This stage is very likely to be controlled by nucleation and/or chemical reaction with an apparent activation energy of 139–161 kJ/mol. The second stage is mainly confined to the reduction of the remaining iron in the spinel and the third stage to the chromium reduction. Solid diffusion of chromium in the oxide phase is the most likely rate-determining step in the third stage with an apparent activation energy of about 410 kJ/mol, while solid diffusion as well as nucleation and/or chemical reaction are very likely to lead to mixed control in the second stage. Besides the possibility of it being able to go into the spinel lattice and release the FeO, lime was also suggested to catalyse the chromite reduction through enhancing the nucleation and/or interfacial reaction in the early stage, and facilitating the solid-diffusion process in the late stage.

References

[1] H.G. Katayama, M. Tokuda and M. Ohtani, Tetsu-to-Hauge, 72 (1986) 1513.
[2] N.F. Dawson, PhD Thesis, University of Natal, Durban, South Africa (1989).
[3] H.G. Katayama, M. Tokuda and M. Ohtani, Trans. ISIJ, 22 (1982) B77.
[4] S. Taneka and D.G.C. Robertson, Proceedings of Pyrometallgy'87, Institution of Mining and Metallurgy, London (1987) p. 937.
[5] P. Weber and R.H. Eric, Metall. Trans., 24B (1993) 987.
[6] J.S.J. Van Deventer, Thermochim. Acta, 127 (1988) 25.
[7] N.S. Sundar Murti, K. Shah, V.L. Gadgeel and V. Seshadri, Trans. Instn. Min. Metall., 98C (1983) 172.
[8] T.R.C. Fernandes, W.E. Lee and T.E. Mitchell, Trans. Instn. Min. Metall., 103C (1994) 177.
[9] Y.L. Ding and N.A. Warner, Kinetics and mechanism of the reduction of carbon-chromite composite pellets with a silica flux (1996) for publishing.
[10] N.A. Barcza, P.R. Jochens and D.D. Howat, Proc. Elec. Furn. Conf. Vol. 1, AIME, Toronto (1971) p. 88.
[11] W.J. Rankin, Trans. Instn. Min. Metall., 78C (1979) 107.
[12] R.J. Fruehan, Metall. Trans, 8B (1977) 279.
[13] Y.K. Rao, Metall. Trans., 2 (1971) 1439.
[14] Y.K. Rao and B.P. Jalan, Metall. Trans, 3 (1972) 2465.
[15] A.R. Branes, C.W.P. Finn and S.H. Algie, J. S. Afr. Inst. Min. Metall., 83 (1983) 49.
[16] J.S.J. Van Deventer and P.R. Visser, Thermochim. Acta, 111 (1987) 89.
[17] J.S.J. Van Deventer, Thermochim. Acta, 112 (1987) 365.
[18] Y.L. Ding, Thesis of MPhil, The University of Birmingham, UK (1996).
[19] E. Uslu and R.H. Eric, J. S. Afr. Inst. Min. Metall., 91 (1991) 397.
[20] O. Soykan, R.H. Eric and R.P. King, Metall. Trans., 22B (1991) 53.
[21] E.T. Turkdogan and J.V. Vinters, Can. Metall. Quart., 12 (1973) 9.
[22] W.J. Rankin, Arch. Eisenhuttenwes, 50 (1979) 373.
[23] O. Soykan, R.H. Eric and R.P. King, Metall. Trans., 22B (1991) 801.
[24] A. Lekatou and R.D. Walker, Ironmaking Steelkmaking, 22 (1995) 378.
[25] A. Lekatou and R.D. Walker, Ironmaking Steelmaking, 22 (1995) 393.